Patterns in a non-local reaction diffusion equation

N.I. Robertson & A.C. Skeldon

Department of Mathematics, University of Surrey, Guildford, Surrey GU2 7XH, UK.

Abstract

The dynamics of a non-local predator-prey model are considered. Unlike many commonly studied two component reaction diffusion systems, this model exhibits steady patterns even when the ratio of the diffusion coefficients for the two species is equal to 1. Furthermore oscillatory solutions with non-zero wavenumber arise. We investigate the neighbourhood of a codimension two point where both a Hopf bifurcation and steady-state bifurcation coincide. The results of a weakly nonlinear analysis are compared with numerical integration of the equations.

Key words: predator-prey, non-local reaction diffusion equations

1 Introduction

Reaction-diffusion equations have been used to model a broad variety of physical phenomena. Some recent models have included non-local terms motivated by neuroscience [1,2] surface chemistry [3], gas dynamics [4] or predator-prey interactions [5–7].

These non-local models are interesting, not least because they show different behaviour from the analogous reaction-diffusion equations with only local terms. For example, in the widely studied local systems with diffusion driven instabilities, such as the Brusselator model, the onset of patterns is only seen if the inhibitor diffuses faster than the activator. Furthermore, when Hopf bifurcation to an oscillatory state occurs, the oscillatory state has no spatial structure (wavenumber $k = 0$) [8]. Investigation of the steady (Turing) bifurcation and the Hopf bifurcation and their interaction has been carried out in a number of chemical models both in one space dimension [9,10] and in two space dimensions [11–13].

In contrast, in two component non-local reaction diffusion systems, patterns can onset even when the activator and inhibitor have equal diffusion coefficients. Hopf bifurcation occurs, but typically for non-zero wavenumber: this kind of bifurcation is sometimes referred to as a wave bifurcation and can result in the appearance of either stable standing or travelling waves. This means that the two component non-local models exhibit at least some of the behaviour seen in three component systems, like that studied in [14].

While previous investigations of two-component non-local reaction diffusion systems have largely focussed on the formation of travelling waves [3] and the dynamics of fronts and defects [4], in this paper we focus on the codimension two point where both Hopf and steady-state bifurcation coincide at a Takens-Bogdanov point. We investigate a particular predator-prey model to illustrate the behaviour that can occur. Such a codimension two point has previously been studied in the context of problems in double-diffusive convection, such as in convection in binary mixtures heated from below in a porous medium [15] and in a fluid [16], in magnetoconvection [17] and in Langmuir circulation [18]. The generic local dynamics expected around such points for systems in one space dimension and for periodic boundary conditions is described by the normal form analysis in [19].

In section 2 we introduce the model and consider the linear stability of the equilibrium state representing coexistence of predators and prey. In section 3 a nonlinear analysis is carried out for the steady-state and the Hopf bifurcation curve and the normal form analysis of [19] used to infer the behaviour local to the Takens-Bogdanov point. The predictions are compared with numerical solutions in section 4 and the results summarised in section 5.

2 Model

The predator-prey model considered is

$$\begin{aligned}
\frac{\partial u}{\partial t} &= u\left(1+\alpha u-\beta u^2-(1+\alpha-\beta)\int_{-\infty}^{\infty}\lambda g(\lambda(x-y))u(y,t)dy\right)-uv+D\frac{\partial^2 u}{\partial x^2}\\
\frac{\partial v}{\partial t} &= av(u-b)+\frac{\partial^2 v}{\partial x^2},
\end{aligned} \tag{1}$$

where u and v are the prey and predator densities respectively. There are six parameters in these scaled equations: a, the growth rate of the predators due to predation; b, the death rate of the predators; D the relative diffusion coefficient of prey to predators; α, a measure of the benefit attained by the prey in aggregation; β, the consequent disadvantages of aggregation due to competition for space; λ, a measure of the localized average of the non-local term. From a biological point of view, for the model to make sense all parameters should be positive. If there is to be a steady spatially uniform state where both predators and prey co-exist then $0 < b < 1$ is also required.

Model (1) with $\beta = 0$ was proposed in [7] as the simplest reasonable predator-prey model that includes non-local terms to model aggregation and the consequent competition for resources. The analysis carried out in [7] suggested that both Hopf and steady-state bifurcation could occur. However, our numerical simulations suggest that in practice the resulting steady or time periodic patterns are not observable. Typically, we found that the trivial state was stable for low values of the bifurcation parameter, α. However, as α was increased, finite time singularities developed in the solution so that the critical value of α for bifurcation to spatially periodic patterns could not be reached. In the single population model investigated in [20], terms analogous to the β terms in equations (1) are included to model the consequent competition for space that results from aggregation. The inclusion of these terms in the predator-prey model both makes for a more realistic model and regularises the behaviour so that for β non-zero finite time singularities do not occur.

The kernel

$$g(\lambda(x-y)) = \frac{1}{2}\lambda e^{-\lambda|x-y|}$$

is considered. This choice has an appropriate qualitative form and has the advantage that by the introduction of an additional variable, w, equations (1) can be transformed from integro-differential equations to the pair of differential equations

$$\begin{aligned}
\frac{\partial u}{\partial t} &= u\Big(1 + \alpha u - \beta u^2 - (1+\alpha-\beta)w\Big) - uv + D\frac{\partial^2 u}{\partial x^2} \\
\frac{\partial v}{\partial t} &= av(u-b) + \frac{\partial^2 v}{\partial x^2}
\end{aligned} \tag{2}$$

along with the constraint

$$0 = \lambda^2(u-w) + \frac{\partial^2 w}{\partial x^2}.$$

It can be shown that solutions of equations (1) must satisfy equations (2) and, conversely, that solutions of equations (2) that are bounded in space are also solutions of equations (1). Consequently, it is reasonable to consider either equations (2) or equations (1), whichever is the more convenient form.

Note that when $\lambda \to \infty$ then $w \to u$ and the model becomes purely local. Conversely, the smaller the value of λ the more important the behaviour at large distances.

Equations (2) have the spatially homogeneous steady-state solutions $(u, v) = (0,0), (1,0), (-1/\beta, 0)$ and $(b, (1-b)(1+\beta b))$ with $w = u$. Only the last of these represents a state where both predators and prey co-exist and hence it is only this state which is of interest. A linear stability analysis shows that this steady-state with co-existence of predators and prey is only stable for some parameter values. Along the line

$$\begin{aligned}\alpha \equiv \alpha_s = & 2\beta b + (\lambda^2 + k^2)\frac{D}{b} + \left(\lambda^2(1 + 2\beta b - \beta) + a(1-b)(1+\beta b)\right)\frac{1}{k^2} \\ & + a(1-b)(1+\beta b)\frac{\lambda^2}{k^4},\end{aligned}$$

there is a steady-state bifurcation where the spatially homogeneous state loses stability to a spatially periodic pattern with wavenumber k. Whereas, along the line

$$\alpha \equiv \alpha_H = 2\beta b + \frac{(1+D)(k^2+\lambda^2)}{b} + (1 - \beta + 2\beta b)\frac{\lambda^2}{k^2},$$

provided

$$k^4 < ab(1-b)(1+\beta b),$$

there is a Hopf bifurcation where the spatially homogeneous states loses stability to a state that is both oscillatory in time and in space with a frequency ω_0 given by

$$\omega_0^2 = ab(1-b)(1+\beta b) - k^4.$$

The line of Hopf bifurcations terminates when it touches the steady-state bifurcation line at $k^4 = ab(1-b)(1+\beta b)$. This point is a Takens-Bogdanov point. Typical linear stability diagrams are shown in Fig. 1. It can be seen that, in an unbounded domain, the first instability can be steady, as would be the case in Fig. 1(a) or oscillatory as in case Fig. 1(c). It is also possible for both oscillatory and steady-state bifurcations to occur simultaneously as shown in Fig. 1(b).

Biologically it is very difficult to determine precise values for the parameters in the model. Throughout this paper we have chosen to fix the values of a, b, β and D and considered how even small changes in the parameter λ effect the dynamics, since it is the parameter λ that determines the importance of non-local behaviour.

3 Nonlinear behaviour

In this section, weakly nonlinear analyses are carried out for the steady-state bifurcation, the bifurcation to standing waves and the bifurcation to travel-

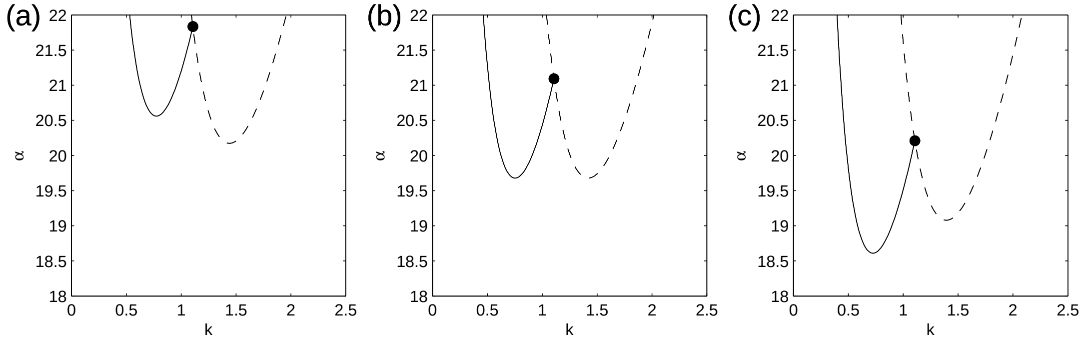

Fig. 1. Linear stability curves in the (k, α) plane. The solid line is the Hopf bifurcation line, α_H while the dashed line is the steady state bifurcation line, α_s . The circle marks the Takens-Bogdanov point. The parameters $a = 1, b = 1/2, \beta = 10, D = 1$ were used and value of λ varied. (a) $\lambda = 1.2$, (b) $\lambda = 1.13387$, (c) $\lambda = 1.05$.

ling waves. This enables us to predict when steady patterns bifurcate supercritically and the relative stability of standing and travelling waves. We also use these calculations to infer what kinds of behaviour local to the Takens-Bogdanov point are possible.

3.1 Steady-state bifurcation

In the vicinity of the steady-state solution $\mathbf{u_0} = (u, v, w) = (b, (1-b)(1+\beta b), b)$, we consider the weakly nonlinear expansions $\mathbf{u} = \mathbf{u_0} + \epsilon\mathbf{u_1} + \epsilon^{\mathbf{2}}\mathbf{u_2}\ldots$, $\alpha = \alpha_s + \epsilon^2\alpha_2 + \ldots$, and the slow time $\tau = \epsilon^2 t$. This kind of weakly nonlinear expansion is standardly applied to systems of partial differential equations to investigate bifurcating branches. There is no difficulty applying these methods to equations (2), even though there is no time derivative for the variable w.

At $O(\epsilon)$ this results in the equations

$$\mathbf{Lu_1} = \mathbf{0}, \tag{3}$$

where

$$\mathbf{L} = \begin{pmatrix} -b(\alpha_0 - 2\beta b) - D\partial_{xx} & b & (1+\alpha_0-\beta)b \\ -a(1-b)(1+\beta b) & -\partial_{xx} & 0 \\ -\lambda^2 & 0 & \lambda^2 - \partial_{xx} \end{pmatrix}.$$

At $O(\epsilon^2)$ we have

$$\mathbf{Lu_2} = \begin{pmatrix} (\alpha_0 - 3\beta b)u_1^2 - u_1 v_1 - (1 + \alpha_0 - \beta)u_1 w_1 \\ a u_1 v_1 \\ 0 \end{pmatrix}. \tag{4}$$

At $O(\epsilon^3)$ we have

$$\mathbf{Lu_3} = \begin{pmatrix} -\partial_\tau u_1 + \alpha_2 b(u_1 - w_1) + 2(\alpha_0 - 3\beta b)u_1 u_2 - (u_1 v_2 + u_2 v_1) \\ \qquad -(1 + \alpha_0 - \beta)(u_1 w_2 + u_2 w_1) - \beta u_1^3 \\ \\ a(u_1 v_2 + u_2 v_1) \\ 0 \end{pmatrix}. \tag{5}$$

Solving the $O(\epsilon)$ problem we find $\mathbf{u_1} = \mathbf{A_{s1}} A(\tau) \cos kx$. where

$$\mathbf{A_{s1}} = \left(1, \frac{a(1-b)(1+\beta b)}{k^2}, \frac{\lambda^2}{k^2 + \lambda^2},\right)^T.$$

The solution at $O(\epsilon^2)$ is $\mathbf{u_2} = (\mathbf{A_{s2}} + \mathbf{B_{s2}} \cos 2kx)\, A(\tau)^2$. The vectors $\mathbf{A_{s2}}$ and $\mathbf{B_{s2}}$ are given in appendix A. Note that these agree with [7] when $\beta = 0$.

At $O(\epsilon^3)$ a solvability condition must be satisfied. This comes from considering the inner product of (5) with the solution to the adjoint of (3). An appropriate inner product is

$$\langle \mathbf{u}, \mathbf{v} \rangle = \int_0^{2\pi/k} \mathbf{u} \cdot \mathbf{v} \quad dx.$$

The adjoint of (3) is then given by

$$\mathbf{L}^* \mathbf{u}^* = \mathbf{0}, \tag{6}$$

where $\mathbf{L}^* = \mathbf{L}^T$. Solving the adjoint equation (6) gives

$$\mathbf{u}^* = \left(1, -\frac{b}{k^2}, -\frac{(1 + \alpha_0 - \beta)b}{k^2 + \lambda^2}\right)^T \cos kx,$$

resulting in a solvability condition of the form

$$\delta_s \frac{dA}{d\tau} = \mu_s \alpha_2 A + \gamma_s A^3,$$

where

$$\delta_s = \frac{1}{k^4}(k^4 - ab(1-b)(1+\beta b)),$$
$$\mu_s = \frac{bk^2}{(k^2+\lambda^2)}$$
$$\gamma_s = \left(A_{s2_1} + \frac{1}{2}B_{s2_1}\right)\left((\alpha_0 - 4\beta b) + \frac{Dk^2}{b} - \frac{a^2b(1-b)(1+\beta b)}{k^4}\right)$$
$$- \left(A_{s2_2} + \frac{1}{2}B_{s2_2}\right)\left(\frac{b+k^2}{k^2}\right)$$
$$- \left(A_{s2_3} + \frac{1}{2}B_{s2_3}\right)(1+\alpha_0-\beta) - \frac{3}{4}\beta, \tag{7}$$

where the A_{s2_i} and B_{s2_i} are the components of the constant vectors $\mathbf{A_{s2}}$ and $\mathbf{B_{s2}}$ that are listed in appendix A.

The coefficient γ_s is negative along the linear stability curves shown in Fig. 1, indicating that the bifurcation to a steady pattern is supercritical in these cases, although this is not true for all possible values of the parameters.

3.2 Hopf bifurcation

3.2.1 Hopf bifurcation: standing waves

In order to perform a weakly nonlinear analysis of the bifurcation to standing waves, we expand $\mathbf{u}$ about the trivial solution $\mathbf{u_0}$ as before, but now on two timescales so that $u_i(x, T, \tau)$ where $\tau = \epsilon^2 t$ and $T = \omega t$. Also, we let $\alpha = \alpha_H + \epsilon^2\alpha_2 \ldots$ and $\omega = \omega_0 + \epsilon^2\omega_2 \ldots$. A similar sequence of problems as for the steady-state bifurcation occurs. Specifically, at $O(\epsilon)$ this gives the equations

$$\mathbf{M u_1} = \mathbf{0}, \tag{8}$$

where

$$\mathbf{M} = \mathbf{L} + \begin{pmatrix} \omega_0\partial_T & 0 & 0 \\ 0 & \omega_0\partial_T & 0 \\ 0 & 0 & 0 \end{pmatrix}.$$

At $O(\epsilon^2)$ we have the same equations as those given in (4) with $\mathbf{L}$ replaced by $\mathbf{M}$. At $O(\epsilon^3)$ we have

$$\mathbf{Mu_3} = \begin{pmatrix} -\partial_\tau u_1 - \omega_2 \partial_T u_1 + \alpha_2 b(u_1 - w_1) + 2(\alpha_0 - 3\beta b)u_1 u_2 \\ -(u_1 v_2 + u_2 v_1) - (1 + \alpha_0 - \beta)(u_1 w_2 + u_2 w_1) - \beta u_1^3 \\ \\ -\partial_\tau v_1 - \omega_2 \partial_T v_1 + a(u_1 v_2 + u_2 v_1) \\ 0 \end{pmatrix} . \quad (9)$$

Solving the $O(\epsilon)$ problem gives $\mathbf{u_1} = \left\{ \mathbf{A_{H1}} \cos kx \, \mathrm{e}^{iT} + c.c. \right\} A(\tau)$ where

$$\mathbf{A_{H1}} = \left(\frac{k^2 + i\omega_0}{a(1-b)(1+\beta b)}, 1, \frac{\lambda^2(k^2 + i\omega_0)}{(\lambda^2 + k^2)(a(1-b)(1+\beta b))} \right)^T$$

The solution at $O(\epsilon^2)$ is then

$$\mathbf{u_2} = \left\{ \left[(\mathbf{A_{H2}} + \mathbf{B_{H2}} \cos 2kx) \, \mathrm{e}^{2iT} + c.c \right] + \mathbf{C_{H2}} + \mathbf{D_{H2}} \cos 2kx \right\} A(\tau)^2.$$

The componenets of the vectors $\mathbf{A_{H2}}, \mathbf{B_{H2}}, \mathbf{C_{H2}}$ and $\mathbf{D_{H2}}$ are given in appendix B.

Again at $O(\epsilon^3)$ a solvability condition must be satisfied. This comes from considering the inner product of (5) with the solution to the adjoint of (3). The appropriate inner product is

$$\langle \mathbf{u}, \mathbf{v} \rangle = \int_0^{2\pi/\omega_0} \int_0^{2\pi/k} \mathbf{u} \cdot \mathbf{v} \quad dx dT.$$

The adjoint of (3) is

$$\mathbf{M}^* \mathbf{u}^* = \mathbf{0}, \quad (10)$$

where

$$\mathbf{M}^* = \mathbf{L^T} - \begin{pmatrix} \omega_0 \partial_T & 0 & 0 \\ 0 & \omega_0 \partial_T & 0 \\ 0 & 0 & 0 \end{pmatrix} .$$

The solution to the adjoint equation (10) is

$$\mathbf{u}^* = \left(-\frac{k^2 - i\omega_0}{b}, 1, \frac{(1 + \alpha_H - \beta)(k^2 - i\omega_0)}{k^2 + \lambda^2} \right)^T \cos kx \, \mathrm{e}^{iT} . \quad (11)$$

The solvability condition is of the form

$$\frac{dA}{d\tau} = \mu_H \alpha_2 A - i\omega_2 A + \gamma_{sw}|A|^2 A,$$

where

$$\mu_H = \frac{bk^2}{2(\lambda^2 + k^2)} \left(1 - \frac{ik^2}{\omega_0}\right)$$

The expression for γ_{sw} is given in appendix C.

3.2.2 Hopf bifurcation: travelling waves

In order to analyse the bifurcation to travelling waves we introduce the travelling wave variable $\xi = \omega t - kx$ and then carry out an analogous weakly nonlinear expansion to that for standing waves. The same equations result for the expansions at first, second and third order and for adjoint but with ∂_T replaced by $\omega\partial_\xi$ and ∂_{xx} replaced by $k^2\partial_{\xi\xi}$.

At first order the solution is similar to that for the standing wave case, namely, $\mathbf{u_1} = \frac{1}{2}\left(\mathbf{A_{H1}}\, \mathrm{e}^{i\xi} + c.c\right) A(\tau)$. At $O(\epsilon^2)$ the solution is given by $\mathbf{u_2} = \frac{1}{2}\left\{\left[\mathbf{B_{H2}} e^{2i\xi} + c.c\right] + \mathbf{C_{H2}}\right\} A(\tau)^2$, where $\mathbf{B_{H2}}$ and $\mathbf{C_{H2}}$ are the same as the coefficients for standing waves and are given in appendix B. The adjoint solution is the same as that for the standing wave problem given in equation (10) and taking the inner product of the equation at third order with the adjoint leads to the solvability condition

$$\frac{dA}{d\tau} = \mu_H \alpha_2 A - i\omega_2 A + \gamma_{tw}|A|^2 A,$$

where γ_{tw} is given in appendix D.

3.2.3 Hopf bifurcation: stability

At the Hopf bifurcation both standing and travelling waves bifurcate simultaneously. As discussed in the context of binary convection in [15], stable waves only result if both $\gamma_{sw} < 0$ and $\gamma_{tw} < 0$. If both are negative, then if $\gamma_{sw} - 2\gamma_{tw} > 0$, standing waves are preferred at onset whereas if $\gamma_{sw} - 2\gamma_{tw} < 0$, it is travelling waves that are preferred. In Fig. 2 γ_{sw}, γ_{tw} and the quantity $\gamma_{sw} - 2\gamma_{tw}$ are plotted along the Hopf bifurcation curves in the region of the Takens-Bogdanov point for the parameter values used in Fig. 1(a) and (c). In both case, γ_{sw} and γ_{tw} are negative. The sign of $\gamma_{sw} - 2\gamma_{tw}$ varies. Immediately in the vicinity of the Takens-Bogdanov point, located at the extreme right of the figure, this parameter is negative in case (a) indicating that it will be travelling waves that are stable at onset near this point. In case (b) it is

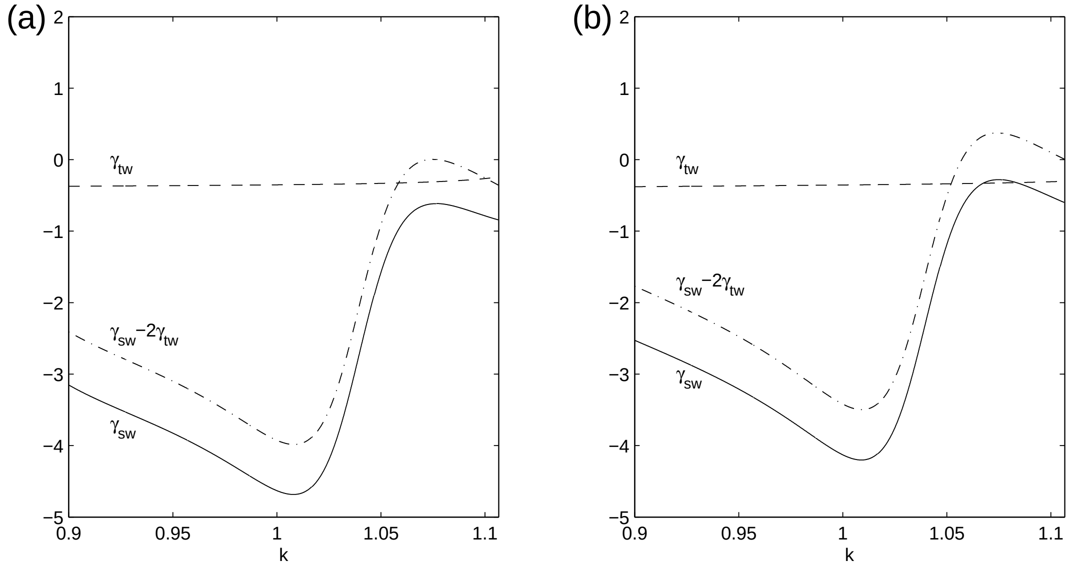

Fig. 2. Cubic coefficients of the Hopf bifurcation as a function of k. The solid line is the coefficient for standing waves, γ_{sw}, the dashed line is the travelling wave coefficient, γ_{tw}. The dot-dashed line is the parameter $\gamma_{sw} - 2\gamma_{tw}$. The parameters $a = 1, b = 1/2, \beta = 10, D = 1$ were used with $\alpha = \alpha(k)$ chosen to lie on the Hopf bifurcation line as shown in Fig 1. (a) $\lambda = 1.2$, (b) $\lambda = 1.05$. The Takens-Bogdanov point occurs at $k = 1.1067$ which is at the extreme right of the horizontal axis.

positive, indicating that it is standing waves that will be stable close to the Takens-Bogdanov point.

3.3 Takens-Bogdanov point

At the Takens-Bogdanov point the dynamics reduce to the normal form [19]

$$\begin{aligned}\dot{V} &= W\\ \dot{W} &= \mu V + \nu W + \Big(A|V|^2 + B|W|^2 + C(V\bar{W} + \bar{V}W)\Big)\,V + D|V|^2 W. \end{aligned} \tag{12}$$

In [19], the solution behaviour local to the Takens-Bogdanov point at $(\mu, \nu) = (0, 0)$ is classified according to the signs of A, D and $M = 2C + D$ and by the ratio M/D. We have not explicitly calculated the values of A, D and M, but from the calculations in sections 3.1 and 3.2, we know their signs since $A \propto \gamma_s, D \propto \gamma_{tw}$ and $M \propto \gamma_{sw}$. For the two cases shown in Fig. 2, both have $A < 0, D < 0$ and $M < 0$. Our analysis of the Hopf bifurcation line showed that for $\lambda = 1.2$ it is travelling waves that are stable at onset close to the Takens-Bogdanov point, by which we can infer that of the possible scenarios outlined [19] this must be case II-. Fig. 3(a) shows the local behaviour predicted by the normal form analysis of [19] in this case. From this it can be

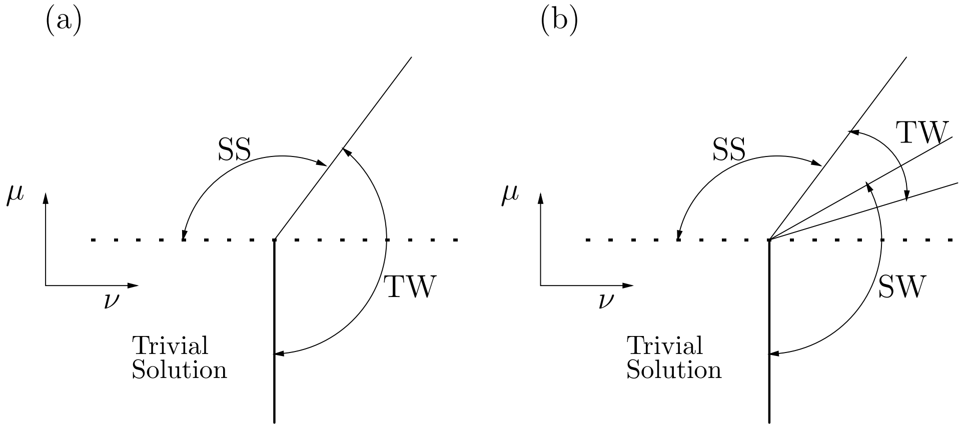

Fig. 3. Stable solutions as given by [19] p. 271. The steady-state bifurcation line is the dashed line at $\mu = 0$. The Hopf bifurcation line is the solid line $\nu = 0, \mu < 0$. The regions labelled SS, TW and SW are the regions where the steady non-trivial solution, travelling waves and standing waves, respectively, are stable. (a) $A < 0$, region II-. (b) $A < 0$, region IV-.

seen that only steady-state and travelling wave solutions are stable local to the Takens-Bogdanov point.

For $\lambda = 1.05$, the analysis of the Hopf bifurcation point indicated that standing waves are stable at the Hopf bifurcation close to the Takens-Bogdanov point. This is consistent with regions III- through to IX- in [19]. As an example, in Fig. 3 we also show the behaviour given by region IV-: the numerical study presented in the next section suggests that this is the relevant region for $\lambda = 1.05$. In this case, stable standing waves bifurcate at the Hopf bifurcation. These are subsequently destabilised and replaced by travelling waves. The normal form analysis shows that there is a branch of unstable modulated waves connecting the standing and travelling wave branches. It is the pitchfork bifurcation to modulated waves that causes the destabilisation/stabilisation of the standing/travelling waves branch.

4 Numerical results

Equations (2) were integrated using a spectral Crank-Nicolson scheme for the linear terms and a pseudo-spectral explicit method for the nonlinear terms. Care was taken to make sure that the equations were integrated for long enough to reach a stable state: close to the bifurcation points the transients take a long time to die away.

Our results are summarised in the bifurcation sets shown in Fig. 4. As consistent with the local analysis at the Takens-Bogdanov point, for $\lambda = 1.2$ the only time dependent states are travelling waves. However, for $\lambda = 1.05$, standing

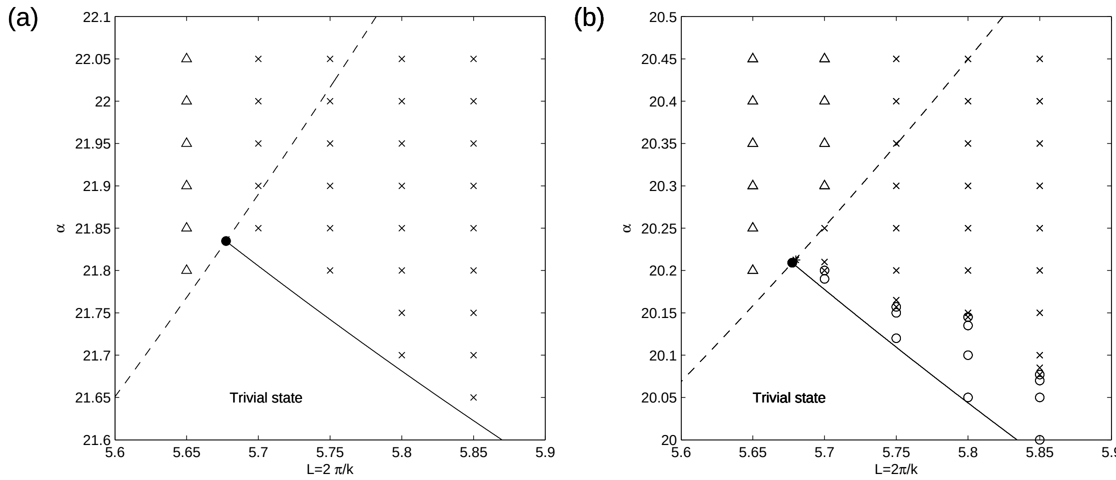

Fig. 4. Bifurcation sets. The parameters $a = 1, b = 1/2, \beta = 10, D = 1$ were used and value of λ varied. (a) $\lambda = 1.2$, (b) $\lambda = 1.05$. Open circles denote standing waves, crosses are travelling waves, triangles steady non-trival state. In some cases both standing waves and travelling waves are stable and these points are marked with both a cross and a circle. The solid line is the Hopf bifurcation line. The dashed line is the steady-state bifurcation line.

waves onset at the Hopf bifurcation point but, on increase of the bifurcation parameter α, these lose stability to travelling waves. There is some hysteresis between this transition: this is seen more easily in Fig. 5 where we plot the maximum and minimum values of $\bar{u} = \frac{1}{L}\int_0^L u(x,t)dx$ against the parameter α for $L = 5.75$ for the two different cases, where $L = 2\pi/k$. This is a convenient measure of the solution and allows us to distinguish between standing and travelling waves. Fig. 5 (a) shows that, for $\lambda = 1.2$, as α is increased there is a continuous increase in the amplitude of $\bar{u}$ from the Hopf bifurcation point. In (b), it is standing waves that onset at the Hopf bifurcation point but these are subsequently destabilised to travelling waves and and the hysteresis between the travelling wave and standing wave branch can be clearly seen. This is consistent with behaviour in region IV- in [19] and illustrated in Fig. 3(b).

Contour plots for typical solutions are shown in Fig. 6. These show examples of standing waves and travelling waves in the prey density u. In each case, as one would expect, the predator density looks similar but the peaks in predator density occur shortly after those in prey density.

5 Summary

In a modified version of the model proposed by [7] we have shown that non-trivial steady-state solutions along with standing waves and travelling waves

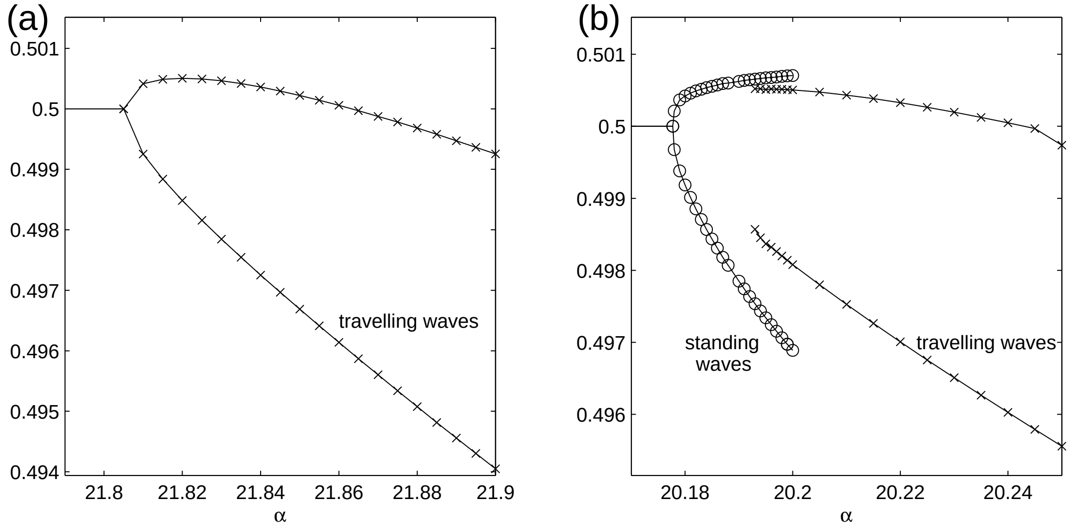

Fig. 5. Bifurcation diagrams. The parameters $a = 1$, $b = 1/2$, $\beta = 10$, $D = 1$, $L = 5.70$ were used. The vertical axis shows the maximum and minimum values of $\bar{u} = \frac{1}{L}\int_0^L u(x,t)dx$. (a) $\lambda = 1.2$. The bifurcation from the trivial solution $u = \bar{u} = 0.5$ occurs at $\alpha_H = 21.805$. (b) $\lambda = 1.05$. The bifurcation from the trivial solution $u = \bar{u} = 0.5$ is at $\alpha_H = 20.178$.

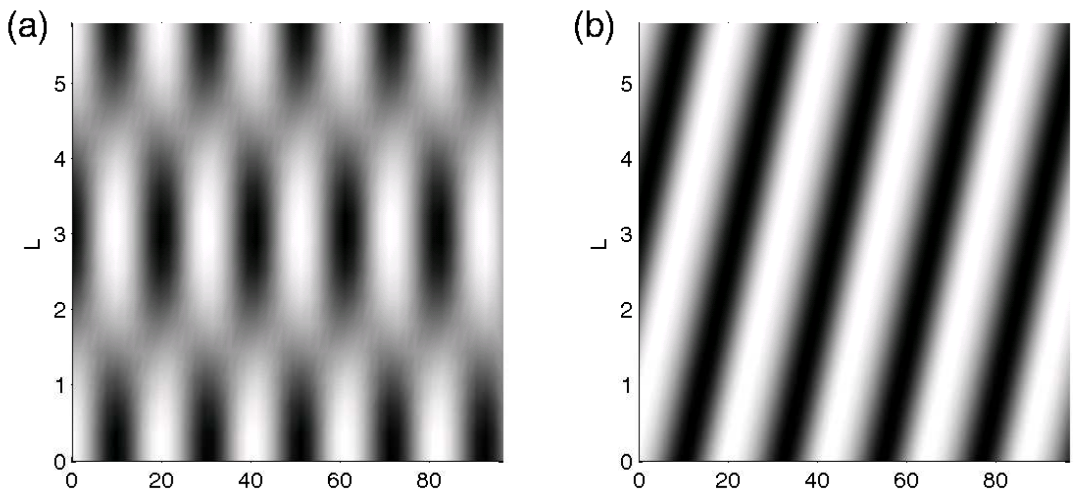

Fig. 6. Contour plots for the prey density u of typical solutions. The parameters $a = 1, b = 1/2, \beta = 10, D = 1, \lambda = 1.05, L = 5.80$ (a) $\alpha = 20.10$, (b) $\alpha = 20.20$.

can occur. Unlike many two-component reaction diffusion equations, there is no need for the ratio of the diffusion coefficients to be different from 1 for patterns to occur. Furthermore, Hopf bifurcations occur for non-zero wave number. We have carried out weakly nonlinear analysis to analyse both the steady and the Hopf bifurcation. These enabled the prediction of the relative stability of standing and travelling waves and by appealing to [19] enabled us to infer the possible behaviours near the Takens-Bogdanov point. Numer-

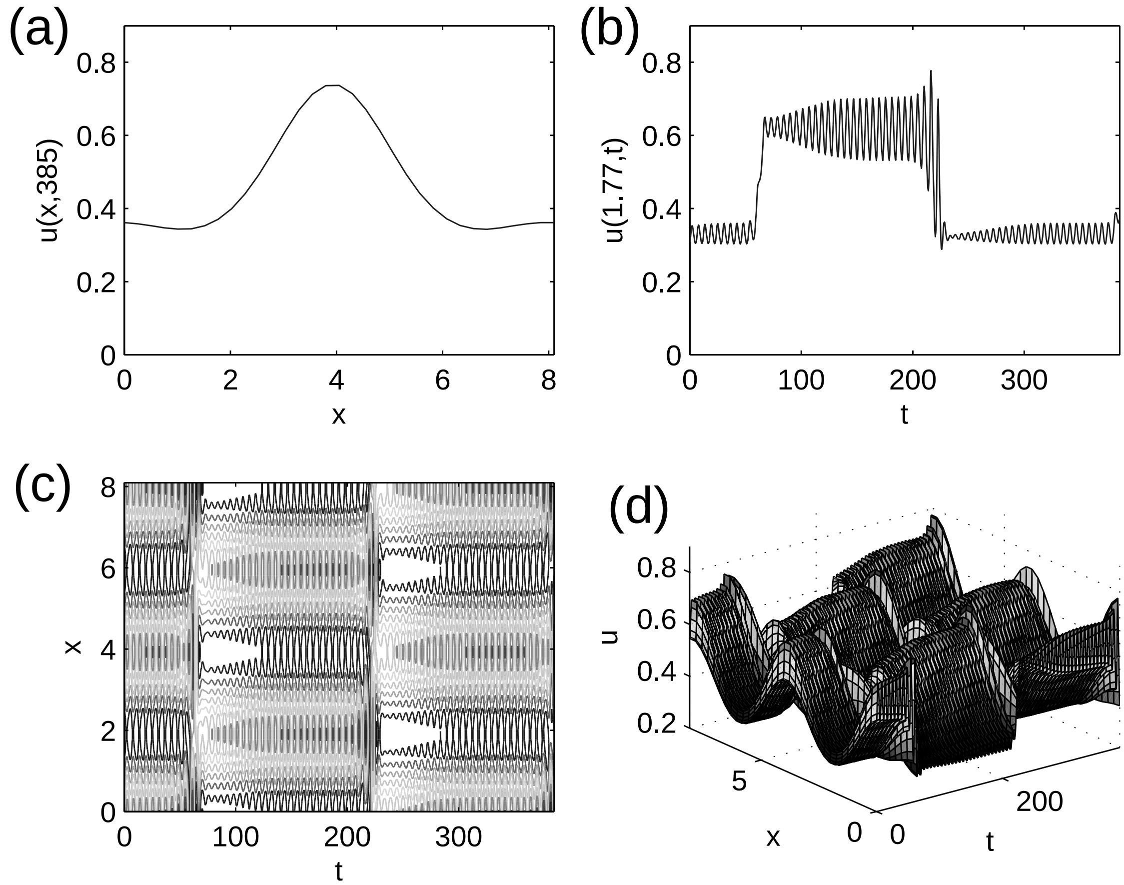

Fig. 7. Numerical solution for the prey density u for the parameters $a = 1, b = 0.47, \beta = 10, D = 2.21, \lambda = 1.95, L = 8.10$ (a) $u(x,t)$ at $t = 385$ as a function of x, (b) $u(x,t)$ for $x = 1.77$ as a function of time, (c) contour plot of u, (d) surface plot of u.

ical solutions of the full equations were consistent with the weakly nonlinear analysis.

Away from the Takens-Bogdanov point there are many other interesting numerical solutions, for example, those shown in Fig. 7. These arise through the 1:2 interaction of a Hopf bifurcation and the steady-state bifurcation and are currently the subject of further investigation.

Acknowledgements

We thank Stephen Gourley for useful discussions on this problem.

References

[1] G. Bordyugov and H. Engel, Creating bound states in excitable media by means of nonlocal coupling, *Phys. Rev. E* **74** (2006) 016205.

[2] N.A. Venkov, S. Coombes and P.C. Matthews, Dynamics instabilities in scalar neural field equations with space-dependent delays, *in preparation*.

[3] M. Hildebrand, A.S. Mikhailov and G. Ertl, Traveling nanoscale structure in reactive adsorbates with attractive lateral interactions, *Phys. Rev. Lett.* **81** (1998) 2602–2605.

[4] E.M. Nicola, M. Or-Guil, W. Wolf and M. Bär, Drifting patterns domains in a reaction-diffusion system with non-local coupling, *Phys. Rev. E* **65** (2002) 055101.

[5] S.R. Choudhury, Analysis of spatial structure in a predator prey model with delay I: linear theory, *SIAM J. Appl. Maths.* **54** (1994) 1425–1450.

[6] S.R. Choudhury, Analysis of spatial structure in a predator prey model with delay II: nonlinear theory, *SIAM J. Appl. Maths.* **54** (1994) 1451–1467.

[7] S.A. Gourley and N.F. Britton, A predator-prey reaction-diffusion system with nonlocal effects, *J. Math. Biol.* **34** (1996) 297–333.

[8] J.D. Murray, Mathematical Biology, Springer-Verlag, Berlin (1989).

[9] A. Rovinsky and M. Menzinger, Interaction of Turing and Hopf bifurcations in chemical systems, *Phys. Rev. A* **46** (1992) 6315–6322.

[10] A. De Wit, D. Lima, G. Dewel and P. Borckmans, Spatiotemporal dynamics near a codimension-two point, *Phys. Rev. E* **54** (1996) 261–271.

[11] B. Peña and C. Pérez-García, Stability of Turing patterns in the Brusselator model, *Phys. Rev. E* **64** (2001) 056213.

[12] L. Yang, A.M. Zhabotinsky and I.R. Epstein, Stable squares and other oscillatory Turing patterns in a reaction-diffusion model, *Phys. Rev. Lett.* **92** (2004) 198303.

[13] W. Just, M. Bose, S. Bose, H. Engel and E. Schöll, Spatiotemporal dynamics near a supercritical Turing-Hopf bifurcation in a two-dimensional reaction-diffusion system, *Phys. Rev. E* **64** (2001) 026219.

[14] A.M. Zhabotinsky, M. Dolnik and I.R. Epstein, Pattern formation arising from wave instability in a simple reaction-diffusion system, *J. Chem. Phys.* **103** (1995) 10306–10314.

[15] E. Knobloch, Oscillatory convection in binary mixtures, *Phys. Rev. A* **34** (1986) 1538–1549.

[16] E. Knobloch and D.R. Moore, Minimal model of binary fluid convection, *Phys. Rev. A* **42** (1990) 4693–4709.

[17] A.M. Rucklidge, N.O. Weiss, D.P. Brownjohn and M.R.E. Proctor, Oscillations and secondary bifurcations in nonlinear magnetoconvection, *Geophys. Astrophys. Fluid Dyn.* **68** (1993) 133-150.

[18] S.M. Cox, S. Leibovich, I.M. Moroz and A. Tandon, Nonlinear dynamics in Langmuir circulations with O(2) symmetry, *J. Fluid Mech.* **241** (1992) 669–704.

[19] G. Dangelmayr and E. Knobloch, The Takens-Bogdanov bifurcation with O(2)-symmetry, *Phil. Trans. Roy. Soc. Lond. A* **322** (1987) 243–279.

[20] J. Billingham, Dynamics of a strongly nonlocal reaction-diffusion population model, *Nonlinearity* **17** (2004) 313–346.

A Second order solution constants for steady-state bifurcation

$$\mathbf{A_{s2}} = \begin{pmatrix} -\frac{a}{2k^2} \\ \frac{1}{2b^2k^2}((1+\beta)ab^2 - \beta b^2k^2 + Dk^4) \\ -\frac{a}{2k^2} \end{pmatrix}.$$

$$\mathbf{B_{s2}} = \begin{pmatrix} \frac{1}{2bk^2 f(\alpha_S, 4k^2)}\left(-a^2b^2v_0 - 4\beta b^2k^4 + 4Dk^6\right) \\ \frac{av_0}{8bk^4 f(\alpha_S, 4k^2)}\left(-a^2b^2v_0 - 4\beta b^2k^4 + 4Dk^6 + abf(\alpha_S, 4k^2)\right) \\ \frac{\lambda^2}{4k^2+\lambda^2}\frac{1}{2bk^2 f(\alpha_S, 4k^2)}\left(-a^2b^2v_0 - 4\beta b^2k^4 + 4Dk^6\right) \end{pmatrix},$$

where $v_0 = (1-b)(1+\beta b)$ and

$$f(\alpha_s, 4k^2) = ab(1-b)(1+\beta b) - 4b(\alpha_S - 2\beta b)k^2 + 4\frac{(1+\alpha_S-\beta)b\lambda^2k^2}{4k^2+\lambda^2} + 16Dk^4.$$

Note that $f(\alpha_s, k^2) = 0$, since this is the equation that defines the steady-state bifurcation curve.

B Second order solution constants for standing wave bifurcation

$$A_{H2_1} = \frac{(k^2+i\omega_0)\left(\omega_0^2\left(\frac{ab}{2} - \beta b^2 + (1+D)k^2\right) + \frac{abk^4}{2} + i\omega_0\left(\omega_0^2 + k^2\beta b^2 - Dk^4\right)\right)}{a^2bv_0^2\left(3abv_0 - 4k^4 - 2i\omega_0 b(1-\beta+2\beta b)\right)}$$

$$A_{H2_2} = \frac{1}{4i\omega_0}\left(\frac{k^2+i\omega_0}{v_0} + 2av_0A_{H2_1}\right)$$

$$
\begin{aligned}
A_{H2_3} =& A_{H2_1}\\
B_{H2_1} =& \frac{(k^2+i\omega_0)\left((2k^4-\omega_0^2+3i\omega_0 k^2)((1+D)k^2-\beta b^2)-(\omega_0^4+k^4)\left(\frac{ab}{2}+2k^2+i\omega_0\right)\right)}{a^2 b v_0^2\left(2(i\omega_0+2k^2)\left(2i\omega_0-b(\alpha_H-2\beta b)+4Dk^2+\frac{b(1+\alpha_0-\beta)\lambda^2}{4k^2+\lambda^2}\right)+abv_0\right)}\\
B_{H2_2} =& \frac{1}{2(2k^2+i\omega_0)}\left(\frac{k^2+i\omega_0}{2(1-b)(1+\beta b)}+av_0 B_{H2_1}\right)\\
B_{H2_3} =& \frac{\lambda^2}{\lambda^2+4k^2}B_{H2_1}\\
C_{H2_1} =& -\frac{k^2}{av_0^2}\\
C_{H2_2} =& \frac{v_0(Dk^2-\beta b^2)+bk^2(1+2\beta b-\beta)}{abv_0^2}\\
C_{H2_3} =& C_1\\
D_{H2_1} =& \frac{k^2(ab+4\beta b^2-4k^2 D)}{av_0\left(-abv_0-4k^2\left(4k^2 D-b(\alpha_H-2\beta b)+\frac{b(1+\alpha-\beta)\lambda^2}{\lambda^2+4k^2}\right)\right)}\\
D_{H2_2} =& \frac{av_0^2 D_{H2_1}+k^2}{4k^2 v_0}\\
D_{H2_3} =& \frac{\lambda^2}{\lambda^2+4k^2}D_{H2_1}
\end{aligned}
$$

where $v_0 = (1-b)(1+\beta b)$.

C Cubic coefficient for bifurcation to standing wave

$$
\begin{aligned}
\gamma_{sw} =& \frac{1}{\delta_H}\Bigg[-\frac{k^2+i\omega_0}{b}\Bigg\{-\frac{(1+\alpha_H-\beta)}{av_0(\lambda^2+k^2)}\Bigg((k^2-i\omega_0)((2\lambda^2+k^2)A_{H2_1}+\frac{\lambda^2(2\lambda^2+5k^2)}{2(\lambda^2+4k^2)}B_{H2_1})\\
&+(k^2+i\omega_0)((2\lambda^2+k^2)C_{H2_1}+\frac{\lambda^2(2\lambda^2+5k^2)}{2(\lambda^2+4k^2)}D_{H2_1})\Bigg)\\
&+\frac{2(\alpha_H-3\beta b)}{av_0}\left((k^2-i\omega_0)\left(A_{H2_1}+\frac{1}{2}B_{H2_1}\right)+(k^2+i\omega_0)\left(C_{H2_1}+\frac{1}{2}D_{H2_1}\right)\right)\\
&-\frac{1}{av_0}\left((k^2-i\omega_0)\left(A_{H2_2}+\frac{1}{2}B_{H2_2}\right)+(k^2+i\omega_0)\left(C_{H2_2}+\frac{1}{2}D_{H2_2}\right)\right)\\
&-\left(A_{H2_1}+\frac{1}{2}B_{H2_1}\right)-\left(C_{H2_1}+\frac{1}{2}D_{H2_1}\right)-\frac{9b\beta(k^2+i\omega_0)}{4a^2v_0^2}\Bigg\}\\
&+a\left(A_{H2_1}+\frac{1}{2}B_{H2_1}+C_{H2_1}+\frac{1}{2}D_{H2_1}\right)\\
&+\frac{1}{v_0}\left((k^2-i\omega_0)\left(A_{H2_2}+\frac{1}{2}B_{H2_2}\right)+(k^2+i\omega_0)\left(C_{H2_2}+\frac{1}{2}D_{H2_2}\right)\right)\Bigg]
\end{aligned}
$$

where $v_0 = (1-b)(1+\beta b)$ and

$$\delta_H = \frac{2i\omega_0(i\omega_0 - k^2)}{abv_0)}.$$

D Cubic coefficient for bifurcation to travelling waves

$$\begin{aligned}
\gamma_{tw} = \frac{1}{\delta_H} \Bigg[& -\frac{k^2+i\omega_0}{b} \Bigg\{ -\frac{(1+\alpha_H-\beta)(2\lambda^2+k^2)}{2av_0(\lambda^2+k^2)} \Big((k^2+i\omega_0) C_{H2_1} + +(k^2-i\omega_0) B_{H2_1} \Big) \\
& + \frac{(\alpha_H - 3\beta b)}{av_0} \Big((k^2-i\omega_0) B_{H_1} + (k^2+i\omega_0) C_{H_1} \Big) \\
& - \frac{1}{2av_0} \Big((k^2-i\omega_0) B_{H2_2} + (k^2+i\omega_0) C_{H2_2} \Big) \\
& - \frac{1}{2} \left(B_{H2_1} + C_{H2_1} \right) - \frac{3b\beta(k^2+i\omega_0)}{4a^2v_0^2} \Bigg\} \\
& + \frac{a}{2} \left(B_{H2_1} + C_{H2_1} \right) \\
& + \frac{1}{2v_0} \Big((k^2-i\omega_0) C_{H2_2} + (k^2+i\omega_0) B_{H2_2} \Big) \Bigg]
\end{aligned}$$

where v_0 and δ_H are given at the end of appendix C.